On-site microbiome study of silica structures in a subterranean Mars analog environment

Martina Cappelletti^{1,2}, Giacomo Broglia¹, Andrea Firrincieli³, Ettore Lopo¹, Alice Checcucci⁴, Daniele Ghezzi¹, Federico Pisani⁵, Freddy Vergara⁵, Bruno Casarotto⁶, Francesco Sauro^{2,6}

- ⁵ Department of Pharmacy and Biotechnology (FaBit), University of Bologna, Bologna, Italy
 - ²La Venta Geographic Exploration Association, Treviso, Italy
 - ³Department for Innovation in Biological, Agro-Food and Forest Systems (DIBAF), University of Tuscia, Viterbo, Italy
 - ⁴Dipartimento di Scienze e Tecnologie Agrarie, Ambientali e Forestali (DAGRI), Università degli Studi di Firenze, Florence, Italy
- 10 ⁵Theraphosa Exploring Team, Puerto Ordaz, Venezuela
 - ⁶Department of Geosciences, University of Padova, Padova, Italy

Correspondence to: Martina Cappelletti (martina.cappelletti2@unibo.it)

Abstract. Amorphous silica deposits found in orthoquartzite caves offer valuable analogues for understanding early life on Earth and potential biosignatures on Mars. This study presents the fully on-site microbial community analysis of silica stromatolite-like structures in the ancient and remote orthoquartzite cave Imawarí Yeutá (Auyan Tepui, Venezuela). Using a portable laboratory setup, we performed ATP-based microbial activity assessments and the full DNA-based analysis workflow directly in the cave, without internet access or high computational resources. The data obtained in the cave were then validated in the laboratory using a standard bioinformatics pipeline, qPCR and Biolog EcoPlate assays. The sequencing results revealed that the microbial communities in the stromatolite differ from other biofilms on the cave floor for the higher abundance of Actinobacteriota (particularly the genus *Crossiella*) and members of Subgroup 13 (Acidobacteriota) suggesting a possible role in the stromatolite formation/development. The ATP-based and Biolog results indicated that the most metabolically active microorganisms are localized in the white layer/colonies at basis of the stromatolite suggesting that the stromatolite development occurs at the interface of this structure with the quartz rock. These findings validate the feasibility of real-time microbial analyses in remote caves with astrobiological interest and provide novel understanding on the microbiological aspects involved in the formation of the silica stromatolites in non-thermal and aphotic environments.

1 Introduction

Amorphous silica deposits are considered modern analogues of siliceous formations originating on Earth during the Precambrian period, providing useful information for studying the evolution of life on our planet. These deposits also have astrobiological interest showing similar composition and morphological characteristics of amorphous silica observed on the surface of Mars by the rover Spirit and by various multispectral cameras onboard of orbital mission (Ruff et al., 2011; Ruff and Farmer, 2016). On Mars, secondary silica deposits could have formed both on the surface and in the subsurface either

through abiotic processes (due to weathering and hydrothermal alteration) or through microbial processes over long periods of time. Given the current environmental conditions hostile to life on the surface of other planets, underground environments represent promising study targets. Indeed, in these sites, the microbial life could have found conditions favourable to proliferation shielded from the high doses of UV and cosmic radiations hitting the martian surface at present time (Boston, 2010). The study of microbial communities interacting with silica and the biological contribution to secondary silica deposits in caves can provide useful information to interpret evidence of possible life forms encrusted in silica deposits on Mars.

Aside of the more common and studied silica sinters in hydrothermal environments, similar non-thermal amorphous silica deposits have been reported during the last two decades in several quartz-rich cave environments (quartz-sandstones, metaquartzites, granites, lava tubes etc.) (Auler and Sauro, 2019; Daza Brunet and Bustillo Revuelta, 2014; Miller et al., 2014; Sauro et al., 2022; Wray and Sauro, 2017). In particular, the exploration of the giant and ancient orthoquartzite caves in the table mountains tepuis of Venezuela and Brazil has led to the discovery of amorphous silica deposits that are novel types of *silica stromatolites* with distinct characteristics, much bigger dimension and spectacular morphologies as compared to those described in volcanic caves (Aubrecht et al., 2008; Lundberg et al., 2018; Sauro et al., 2018). The formation of these deposits in geochemically stable, non-thermal and aphotic environments is associated with microbial activities that are still mostly unknown (Ghezzi et al., 2021; Sauro et al., 2018).

In recent years, there has been a growing interest in the development of cost-effective, portable detection systems suitable for various in situ applications, including environmental monitoring, pathogen detection in clinical and food safety contexts, and astrobiological investigations in remote and extreme environments (Quintela et al., 2022). Among them, nucleic acid-based analyses provide information on the presence and abundance of specific microbes that can be involved in the interaction with the surrounding setting and with its modification. Recent progress in sequencing technologies have allowed to carry out DNA sequencing outside of the laboratory allowing microbiome analysis to be conducted in situ. The advantages of in situ DNA analyses include to avoid sample degradation, to limit problems with transportation and to allow field-based pre-screening for informed sample selection. Furthermore, DNA sequencing is also seen as possible method to detect life during astrobiology missions and in extraterrestrial settings (Maggiori et al., 2020; Mojarro et al., 2019).

In this work we carried out on-field microbiological analyses of the silica stromatolite-like structures, which are biosignatures with astrobiological interest, directly in the cave Imawari Yeuta. We carried out the entire DNA-based analysis workflow including DNA extraction, amplification, sequencing, data analysis and results visualization directly in the cave by applying a tailored bioinformatic pipeline that we developed to process sequencing data in under 20 minutes (per sample) without internet access or high computational resources. A portable ATP detector was also used to assess microbial activity levels in the cave that were then validated though qPCR and Biolog assay in the lab. The results provided novel understanding on the microbial communities and activities characterizing silica stromatolites development.

2 Study area

2.1 The Imawari Yeutà cave system

Imawarí Yeutá is an ancient and pristine orthoquartzite cave located on the table-top mountain Auyan Tepui in Venezuela. The cave is located at approximately one hundred meters of depth below the tepui plateau surface (between 2000 and 1900 m above sea level). The cave has been carved in at least 20-30 million years by erosion and weathering (arenization) of infiltrating waters. The geological setting and speleogenetic processes of the cave have been extensively described previously (Mecchia et al., 2014; Sauro, 2014; Wray and Sauro, 2017). The cave presents stable physical-geochemical conditions, with a constant temperature between 15 and 18 °C and acidic waters with a pH ranging from 3 to a maximum of 6.1 (Mecchia et al., 2014). After few meters from the entrances, the cave is characterized by a total absence of light. Air flows and water streams are concentrated along few main branches, while extensive areas of the cave are abandoned by flowing waters since millions of years. Most of the silica stromatolites are found in these quiet environments where very limited air and water exchanges result in canonical oligotrophic conditions, with low nutrient availability and scarce organic carbon sources. In this regard, the innermost zones of quartzite caves in the tepui mountains are considered oligotrophic ecosystems, with organic nutrient concentrations close to undetectable levels (as reported in (Barton et al., 2014; Ghezzi et al., 2022; Mecchia et al., 2014; Sauro et al., 2018)). Unlike the external surface, which receives constant inputs from soils and vegetation, the cave interior is deprived of external nutrient sources and lack primary production associated to light-driven photosynthesis.

80

2.2 Cave silica stromatolites

Silica stromatolites are usually well-known in hot-spring sinters (Konhauser et al., 2004) where ascending hydrothermal waters generated in deep-hot reservoirs contains high quantity of dissolved silica (Gunnarsson and Arnórsson, 2000), and supersaturation is caused by cooling and evaporation at the ~100-70 °C spring temperature. However, it is important to underline that there is no affinity between quartz-rich cave environments and hot-spring conditions. In Imawarí Yeutà cave the temperature is nearly constant throughout the year, atmospheric pressure is in the same order of surface pressure and SiO₂ solubility in fractures or cave walls (i.e. where silica is mostly dissolved) equals SiO₂ solubility at the surface (Mecchia et al., 2014). In addition, subsurface silica stromatolites in the caves of the tepui table mountains of the Guyana Shield are always forming over boulders or along the walls, in wet or dry conditions, but never submerged in aquatic environments. The stromatolitic morphology and the peculiar geochemical conditions suggest that amorphous silica precipitation is also mediated by microbiological activities (Sauro et al., 2018).

Imawarí Yeutá and other cave systems explored in the Venezuelan tepuis host a wide variety of silica stromatolites and speleothems (Fig. 1 (Sauro et al., 2013)) showing a variety of morphologies (bulbous-, columnar-, mushroom-, egg-and corallike forms), most of them characterised by thin stromatolitic layers constituted of amorphous silica (amorphous gels and Opal-A) encrusting biological components (cells, filaments, EPS, etc.) (Fig. 1, Fig. 2).

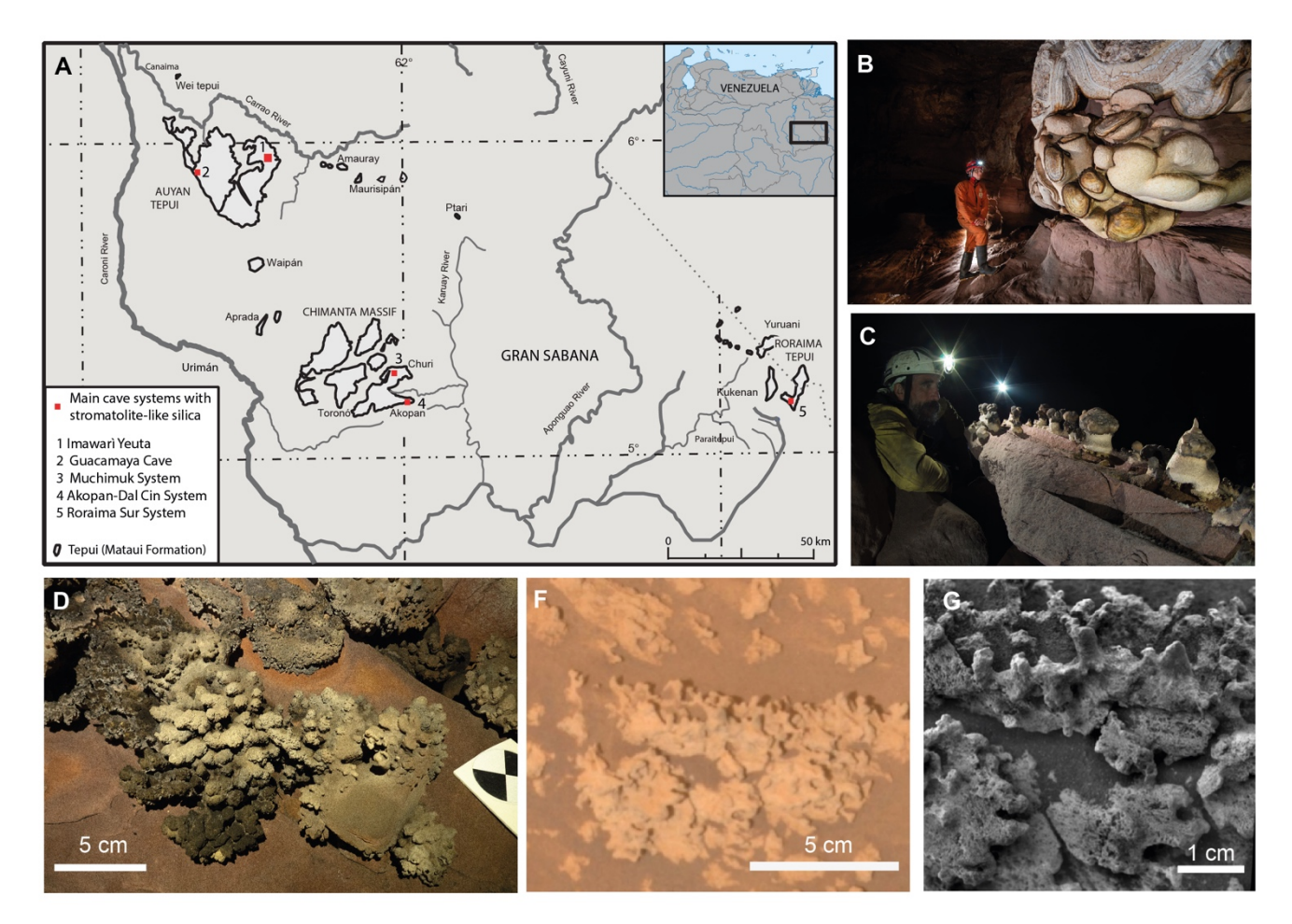


Figure 1: A) Location of Imawari Yeuta and other cave systems in quartz-sandstones where the presence of silica stromatolite-like deposits have been reported (Wray and Sauro, 2017); B-C) Different types of silica speleothems growing on quartz-sandstone walls and boulders (photos Vittorio Crobu – La Venta). D) Silica stromatolitic digitate structures on the floors of Imawarí Yeuta, showing similar morphologies to opaline silica found by the Rover Spirit in the Home Plate outcrop on Mars (F, G; from Ruff and Farmer, 2016).

100

105

In some cases, coralloid and branched stromatolites are morphologically similar to the silica deposits found in the Home Plate site analyzed by the Spirit rover on Mars (Fig. 1 D-E-F). For this specific in-situ analysis study we have focused on one of the more classical type of stromatolites, described by (Aubrecht et al., 2012) as mushroom- or globular-shaped stromatolites with chalky peloidal layers, white on the surface and interior, with greyish darker and harder material caps. These deposits formed over deeply weathered orthoquartzite boulder or along ledges on the walls (Fig. 1).

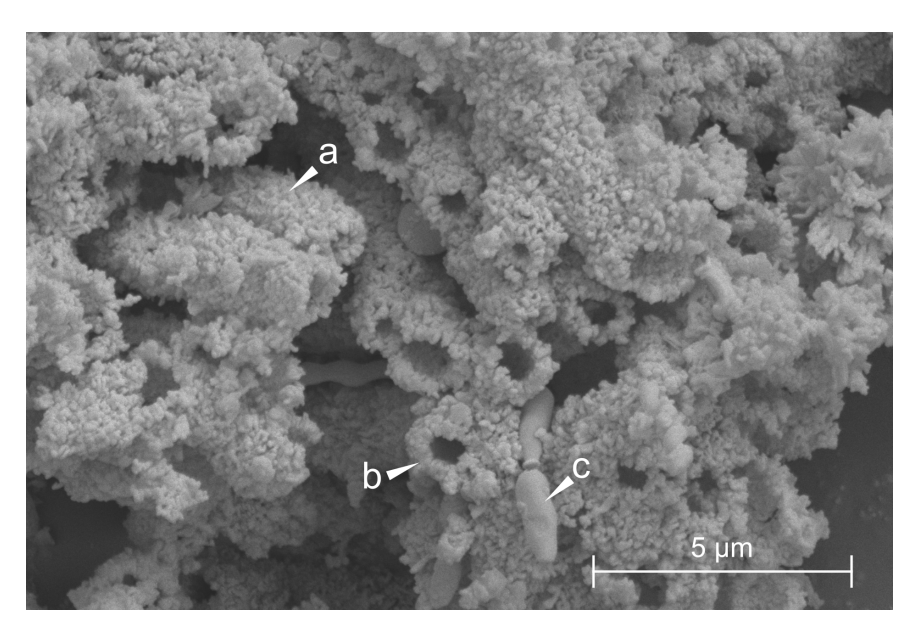


Figure 2: SEM/FESEM image of a sample collected from the white paste of a silica stromatolite-like formation in Imawarí Yeutá. Arrows indicate a) botryoidal masses of precipitated amorphous silica, b) the section of a tubular cast, c) a bacterium-like structure

In order to test and compare the results with different cave niches, the study has also analyzed two patinas on the floors (white and yellow) not associated with stromatolites but with typical microbial colonies growth (**Table S1**).

115 3 Study area

120

125

3.1 Hyperspectral imaging for amorphous silica identification

The hyperspectral signature of the stromatolite was obtained with a Headwall Photonics Micro-Hyperspec push-broom camera, with a spectral range 900 to 2500 nm, 170 spectral bands, 384 spatial bands, FWHM 10 nm. The set-up housing for hyperspectral acquisitions consists of a camera holder and a high-precision 20 x 20 cm motorised stage, while the illumination is equipped with a 150 w tiltable halogen lamp with a frosted glass diffuser and reflector. A Spectralon (Labsphere, Inc.) with a reflectivity of 99% was used as a white reference for radiance conversion.

3.2 Sampling and laboratory setting

A field laboratory was set up under a 3x3 m tent around 200 meters from the entrance of the cave. The chosen area consisted of an isolated cave recess, distant from the main routes of the cave that connect the entrance with the base camp located inside. Further, in this area there were no water flows or drippings, and no wind currents. The tent was properly closed so as not to allow insects or other small animals to enter. The laboratory was equipped with a table and common laboratory instruments essential for basic molecular experimental procedures (pipettes, tips, microtubes). Large instrumentation included a vortex

(Vortex-Genie 2), the Bento Lab portable PCR workstation to conduct DNA extraction, 16S rRNA amplification, and amplicon visualization through gel electrophoresis, the MinION Mk1C to carry out DNA sequencing, and a high-performance computer for in situ data analyses (Lenovo laptop with 4 CORE, 32 Gb RAM, 1 TB hard-disk).

Sampling was performed using sterile procedures. Samples were collected in areas of the cave located approximately 350 meters in a straight line from the temporary laboratory, corresponding to about 650 meters along the actual path. Samples were collected inside microtubes that were transported to the temporary laboratory and immediately processed for total microbial DNA extraction.

Electricity was provided through a Honda 1 Kw power generator installed outside of the cave with a cable running for more than 200 meters to the interior until reaching the field laboratory.

3.3 Bioluminometer for ATP-based measurement in the cave

135

150

155

160

Bioluminometer (RingBioTM) is a hand-held instrument which allows the quantification of adenosine triphosphate (ATP) that is directly proportional to the metabolic activity of microbial cells present in a sample. This type of analysis was used to have indications on the microbial activity in cave samples/areas. For this purpose, the selected areas were swabbed, then the swab was placed inside the ATP detector/bioluminometer and the test activated. The assay is based on the use of an enzymatic reaction constituted by the "luciferase - luciferin system" that produces an amount of light that is directly proportional to the amount of ATP present in the sample and is expressed as Relative Light Units (RLU). The test was repeated three times by scrubbing in a standardized way (areas of around 1 x 1 cm²) three different areas of the same type of sample under analysis.

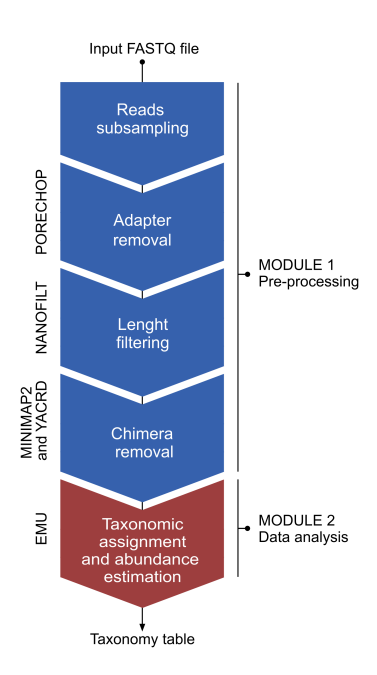
3.4 DNA extraction, 16S rRNA gene amplification, barcoding and sequencing in the cave laboratory

Total microbial DNA extractions were carried out using the DNeasy PowerLyzer PowerSoil Kit (Qiagen) as previously described (Ghezzi et al., 2022). Since we did not have an analytical balance to measure the amount of sample to extract (up to 250 mg per sample according to the manufacturer's protocol), we arbitrarily added an amount of sample that filled approximately one quarter of the volume of the Qiagen tube with the PowerBead solution. 1 μL of the extracted DNA was used to perform amplification reactions using the Bento Lab PCR Workstation. Full-length 16S rRNA genes (V1-V9) were amplified in 50-μL reaction mix using 27F (5'-AGAGTTTGATCMTGGCTCAG-3') and 1492R (5'-CGGTTACCTTGTTACGACTT-3') primer pair with 16S Barcoding Kit (SQK-RAB204, Oxford Nanopore Technologies, Oxford, UK) and the Phanta Max Super-Fidelity DNA Polymerase (Vazyme) following the manufacturer's protocol. The amplifications were carried out using the following settings: initial denaturation for 1 min at 95 °C; 30 cycles of denaturation for 15 sec at 95 °C, annealing for 15 sec at 56 °C, extension for 90 sec at 72 °C; final extension for 5 min at 72 °C. PCR reactions were checked through gel electrophoresis. Barcoded amplicons were pooled together to yield a final amount of 1 μg of multiple barcoded DNA and processed for end repair and dA-tailing using the NEBNext Companion Module for ONT Ligation Sequencing (New England Biolabs, E7180S). The library was purified using AMPure XP beads (Beckman Coulter Diagnostics, USA, CA) and loaded onto an electrophoresis gel for approximate quantification. After priming of the flow cell

with the Flow Cell Priming Kit (EXP-FLP002), 100 fmol (equivalent to approximately 100 ng for 16S rRNA amplicons) of the purified DNA library was loaded onto an R9.5 flow cell (Flow Cell Mk I, R9.4, FLO-MIN106) according to the manufacturer's instructions. Finally, a sequencing run of approximately 2 hours was performed, with real time basecalling enabled, and carried out directly in situ using the MinKNOW software.

3.5 Bioinformatic analyses: pipelines applied in the cave and in the laboratory and statistical analyses of the sequencing results

170 Cave procedure pipeline was specifically created for the in-situ analysis of 16S rRNA gene sequences base called using the "fast" mode basecalling model through the MinKNOW software integrated in the MinION Mk1C sequencing device. The main objective was the implementation of a bioinformatic pipeline able to complete the analysis of 16S rRNA sequences for each sample in less than 20 minutes (due to electrical power limitation) and without internet connection. The pipeline was entirely based on bash (unix) and the general workflow is illustrated in Figure 3.



165

175

180

Figure 3: Flowchart showing the main bioinformatic steps of the Cave pipeline

The pipeline consists of two modules, i.e., a pre-processing module and a classify module. In the pre-processing module, the raw reads are processed through the following steps: i) random subsampling at 25% with reformat.sh from BBMap package v38.98 (https://sourceforge.net/projects/bbmap/), ii) adapter removal by Porechop v0.2.4 (https://github.com/rrwick/Porechop), iii) length (1200 − 1800 bp) and quality (≥9) filtering using Nanofilt v2.6.0 (https://github.com/wdecoster/nanofilt), iv) chimera removal through yacrd vIvysaur using recommended settings for ONT

data (https://github.com/natir/yacrd). The second module enabled taxonomy classification and calculation of taxa abundances

of the filtered reads against the prebuilt SILVA database v138.1 using the EMU classifier v3.4.5 (Curry et al., 2022). The time
requirement for the entire workflow was under 15 minutes, considering approximately 25,000 to 30,000 reads processed for
each sample after the initial subsampling at 25%.

For the lab procedure, the same data analysis workflow was followed except for the base calling modality and the subsampling. The reads processed by the lab procedure were base-called using "super accurate" mode with Guppy v6.11. This mode requires access to a machine with a GPU to complete the basecalling within an acceptable timeframe. Such GPUs are often available on HPC nodes whose access requires an internet connection or in high-performing laptops that still would require several hours to complete the basecalling. The direct comparison between the two pipelines is indicated in Table S2.

The abundance data generated from EMU were combined to produce sample-wise taxon-specific abundance tables at the Phylum, Class, Order, Family, and Genus levels, with taxa showing abundances below 1% grouped under the category 'others'. Visualisation of compositional data through bubble plots (Figure 11; Figure S2) was performed using ggplot.

Alpha and beta diversity metrics were calculated using the R package Vegan v2.6.4. The R package ComplexHeatmap and ggplot2 were used to visualise Genus-level Bray-Curtis dissimilarities between stromatolite (ST-w and ST-b) and biofilm (D-w, P-w, P-y) samples (Figure 10: Figure S1)

The goodness-of-fit of taxonomic distributions at different levels between the lab and cave pipelines was assessed using a Chi-square test, implemented through the chisq.test function of the R stats package (v3.6.2). This statistical test allows the assessment of whether the distribution of taxa in the cave_pipeline deviated significantly from that of the lab_pipeline. The shell scripts used to process sequencing data into EMU abundances, as well as the R scripts used for statistical analyses, beta and alpha diversity analyses, and visualisation of the results, are available on Figshare doi: 10.6084/m9.figshare.29514197.

3.6 Bacterial quantification through qPCR

190

195

200

205

210

The quantification of the community 16S rRNA genes was conducted in triplicates through qPCR by using the CFX96 Real-Time PCR Detection System (Bio-Rad Laboratories Inc., Hercules, USA). qPCR reaction mixes were prepared in a final volume of 10 μ L containing 1 μ L of the extracted DNA, universal primers 926F and 1026R (300 nM each) (Ghezzi et al. 2024), and 1x AceQ qPCR SYBER Green Master Mix (Vazyme Biotech Co., Nanjing, China). The standard curve (R² > 0.99) was generated by using serial dilutions of known amounts of 16S rRNA gene PCR products of Escherichia coli as template. Finally, DNA amplification was carried out using the following thermocycling conditions: 95 °C for 5 min, 40 cycles of 95 °C for 10 s and 60 °C for 30 s.

3.7 Metabolic activity analyses through Biolog Ecoplate assay

To assess the metabolic activity and the carbon source utilization profile of microbial communities, samples isolated from different stromatolite-like structures were screened using Biolog Ecoplate (Biolog, Inc., Hayward, CA, USA). The 96-well microplates are composed by three replicate sets of 31 lyophilized relevant carbon substrates together with a tetrazolium redox

dye (Insam, 1997). Ecoplates carbon sources can be grouped by chemical class (carbohydrates, carboxylic acids, complex carbon sources, amino acids, and amines, as listed in **Table S3**). Microbial substrate utilization is indicated by color changes of the tetrazolium redox dye in each well. This technology relies on active cell metabolism, where the dye is reduced by NADH produced during respiration, leading to the formation of the purple compound formazan. 0.1 g of sediments were first resuspended in 10 mL of 0.1% Na₂H₂P₂O₇ (pH 7), shacked on a tilting table for 2 hours to favour cell detachment and filtered through Labor filter paper (50 x 50 cm, 67 g/m²) to avoid interference with spectrophotometric reading. 150 μL of the resulting suspension were then added to the wells of the microplates and incubated in the dark at 20°C. Absorbance changes were monitored during the incubation at a wavelength of 595 nm using an EnSpire Multimode Plate Reader (Perkin Elmer, USA), which recorded the level of substrate consumption represented by colour change in every well. Two incubation periods were selected, i.e., 5 and 14 days. The first one corresponds to the time that is typically used in Biolog experiments, while the second one was selected because previously adopted in studies analysing microbial metabolic activities in cave samples using Ecoplates (O'Connor et al., 2021). After inoculation, the Ecoplates were sealed with Parafilm and placed inside sealed containers containing water-soaked absorbent paper to maintain humidity to avoid volume loss due to dryness. The metabolic activity value (MAV) was represented by the recorded OD₅₉₅ for every timepoint.

4. Results

220

225

230

240

245

235 4.1 Silica stromatolite-like structures as potential biosignatures with astrobiological interest

The samples analysed in this study were collected from different areas of stromatolite-like structures (representative image of the stromatolites are shown in Figure 1) that were selected depending on their macromorphology, based on previous reports of silica stromatolites in the caves of the tepuis (Aubrecht et al., 2012; Sauro et al., 2014).

Moreover, three additional samples were collected from microbial biofilms that were present on the floor of the cave. The sample description is reported in Table S1.

The hyperspectral signature in the SWIR range 1.0 to 2.4 (Fig. 4) confirm the amorphous silica composition and the similar absorptions bands at 1.4, 1.9 and 2.25 observed by satellite cameras (CRISM) in several proposed amorphous silica outcrops on the surface of Mars (Smith et al., 2013). This peculiar composition and spectral characteristics suggest that subsurface silica stromatolites could be also potential biosignatures to investigate on Mars, alongside with the already proposed silica sinters in hydrothermal conditions (Ruff et al., 2011; Ruff and Farmer, 2016).

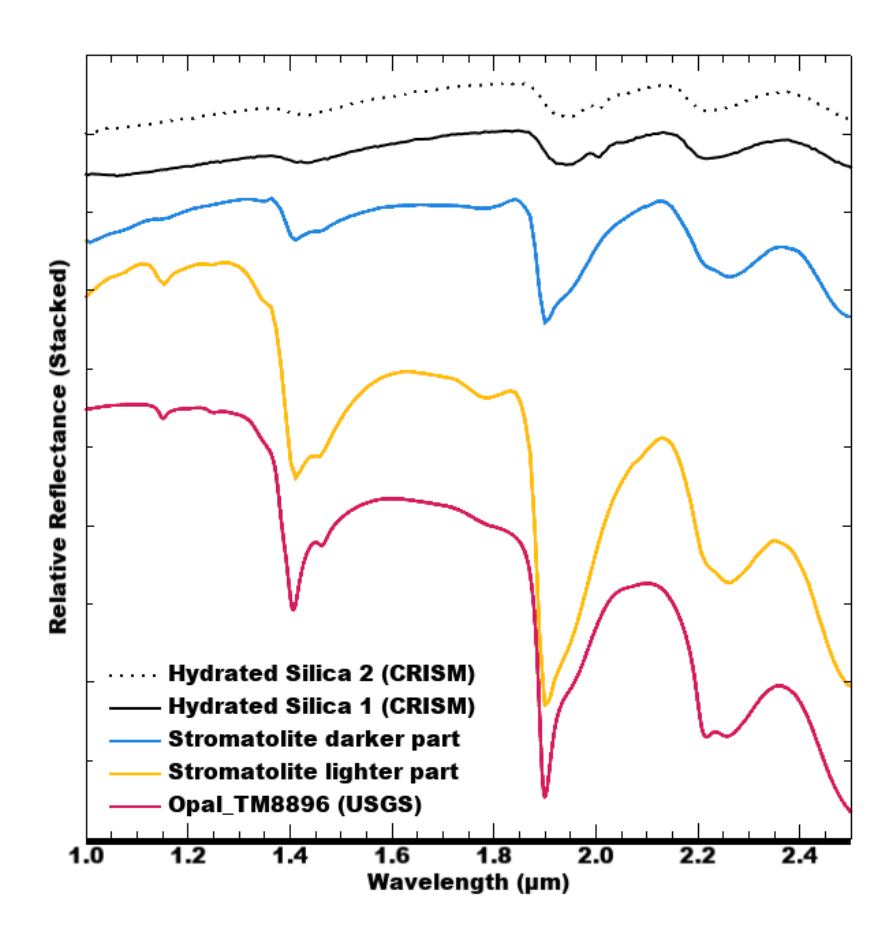


Figure 4: Hyperspectral analysis of the stromatolite samples. Stromatolite darker part is ST-b; stromatolite lighter part is ST-w.

4.2 Microbial activity and abundance in silica stromatolite samples

250

255

4.2.1 On-site ATP detection in the stromatolite-associated samples

For microbial activity analysis 3 samples were collected from the two representative areas of the silica stromatolite, i.e. the white paste at the interface between the quartz rock and the stromatolite-like structure and the blackish/greyish patina on the top of the stromatolite. The results indicated that the white microbial colonies/biofilms at the interface between the quartzite rock and the stromatolite showed the highest activity value indicating the presence of metabolically active microbial communities in the stromatolite region that is in contact with the quartzite rock (Fig. 5). On the other hand, microbial biomass on the top of the stromatolite (at the level of the black/greyish patina) showed the lowest activity.

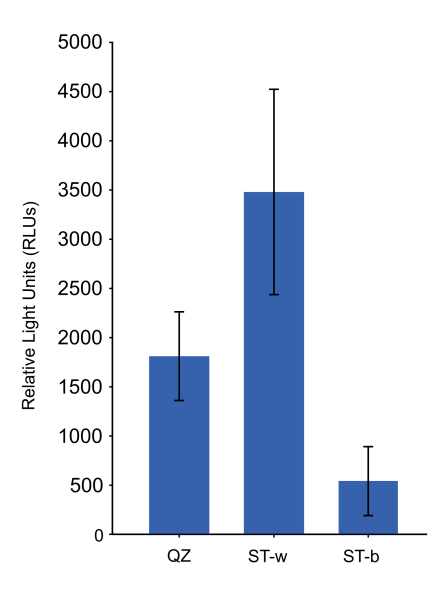


Figure 5: Microbial metabolic activity detected through bioluminometer in the different silica stomatolite samples. QZ = unmodified quartz rock, ST-w=white part of the stromatolite, ST-b= black/greysh patina on the top of the stromatolite

4.2.2 Microbial quantification and metabolic activity analyses in the lab

The quantification of bacterial biomass was carried out in the lab by using qPCR targeting the 16S rRNA gene in the same

DNA samples that were processed in the cave for DNA extraction. The results showed a higher number of copies of 16S rRNA

gene (of around one order of magnitude) in the white colonies/biofilm samples collected at the interface between the rock and
the stromatolite as compared to the samples collected from the top part of the stromatolite (Fig. 6).

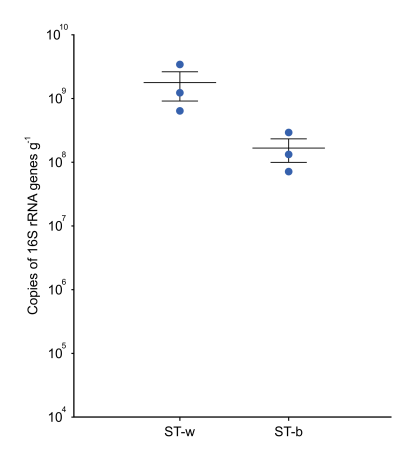


Figure 6: Quantification of the prokaryotic cell biomass present in ST-w (the white part of the stromatolite) and ST-b (the black/greysh patine on the top of the stromatolite) through qPCR targeting the 16S rRNA gene. The abundance is expressed as

number of copies of 16S rRNA per gram of sample. A t-test was performed and the results indicated that the difference was not statistically significant (p-value = 0.133).

The analysis of the metabolic activity was conducted in the lab by using microplates EcoPlate by Biolog which allow the measurement, and the quantification of microbial metabolism based on the detection of reducing power (in the form of NADH) produced by the cells during the incubation with different substrates and their consumption. Two incubation periods were selected, i.e., 5 and 14 days. The longer incubation period (14 days) yielded the same patterns observed at 5 days, but with higher levels of metabolic activity; therefore, only the 14-day results are reported in Figure 7. The results showed that the microbial community associated to the white colonies/patina of the speleothem reaches a higher metabolic activity value (MAV) in terms of number of substrates consumed as compared to the black patina. Figure 7 shows the functional metabolic diversity across the various biochemical categories listed in Table S3. The comparison of metabolic profiles indicated that the microbial community in ST-w generally showed the capacity to metabolize a higher number of substates and at higher activity level as compared to ST-b. Considering the substrate categories, the microbial communities in the two stromatolite samples exhibited similarities in the utilization of compounds belonging to the carbohydrate and polymer categories, maintaining a uniform trend in term of MAV range in most of the substrates tested. The most evident exceptions can be observed on the substrates D-cellobiose, pyruvic acid methyl ester and α-D-lactose where ST-w exhibited significantly higher metabolic activity as compared to ST-b. Conversely, the microbial community in ST-w displayed higher activity and a broader range of metabolized compounds in the amino acid and amine categories.

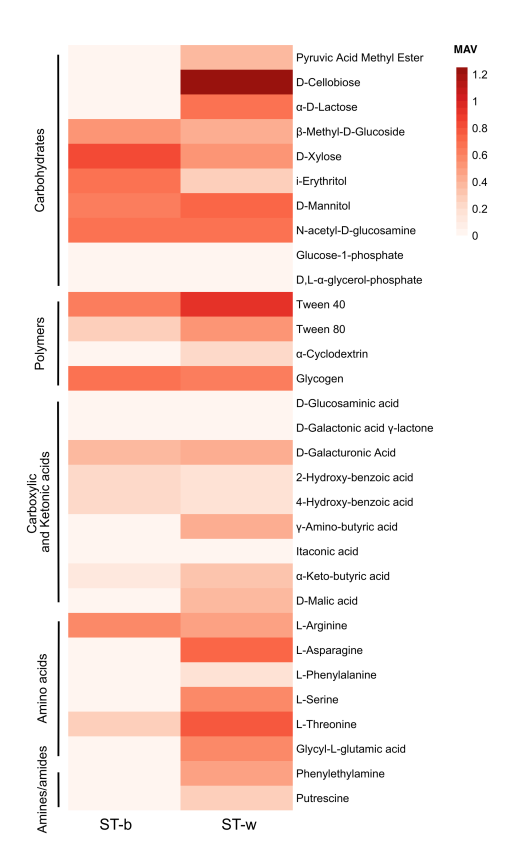


Figura 7: Heatmap plot of Metabolic Activity Value (MAV) in the black patina (ST-b) and in the white part of stromatolite (ST-w). The MAVs obtained on different carbon sources after 14 days of incubation at 18 -20 °C are indicated.

4.3 Microbial community diversity and composition

295 4.3.1 On-site metabarcoding sequencing analyses and in-lab validation

The two samples from the stromatolite (ST-b and ST-w) were processed directly in the cave for DNA extraction and sequencing (using Oxford Nanopore sequencing technology) together with other three biofilm samples representative of microbial colonization on the cave floor (Fig. 8, Table S1).

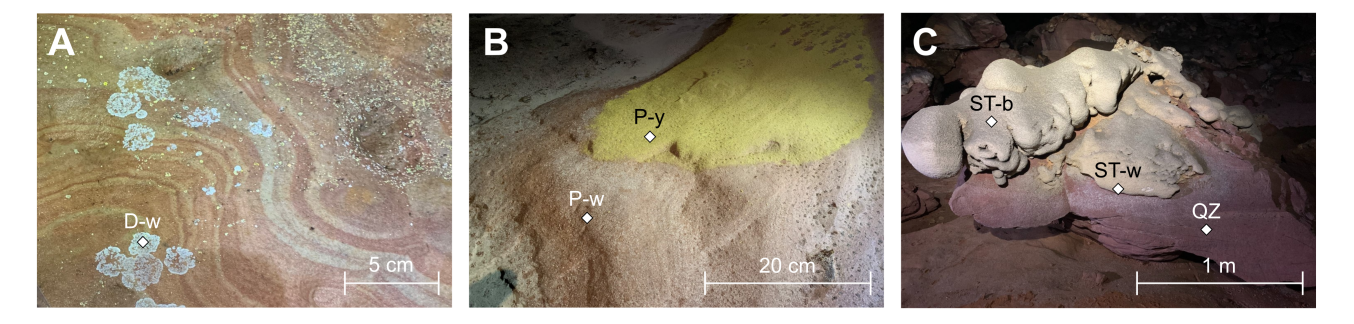


Figure 8: Picture of the samples collected in Imawarí Yeutá and processed for DNA extraction and sequencing in cave. A) White dendritic spot (D-w); B) Yellow (P-y) and white (P-w) biofilms colonizing the quarzite floor of the cave; C) White paste (ST-w) of the silica stromatolite and the black patina (ST-b) covering the top of it

In the cave, after the sequencing run, the sequencing results were processed by using the cave_pipeline to analyse and visualize in situ the microbial community composition (**Fig. 9**).

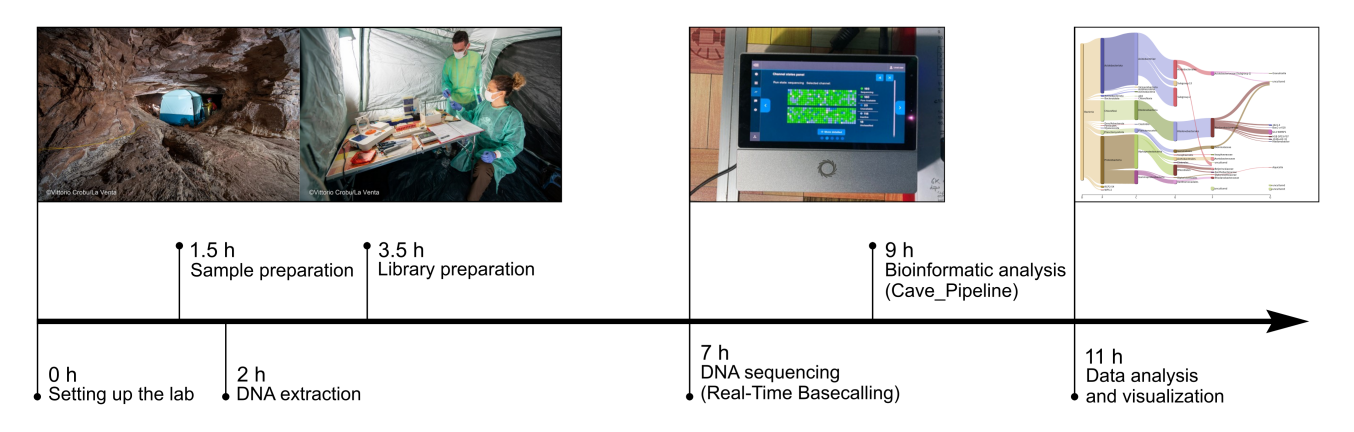


Figure 9: Timeline of the fully on-site procedure applied to conducted DNA-based analysis of microbiological samples in the cave

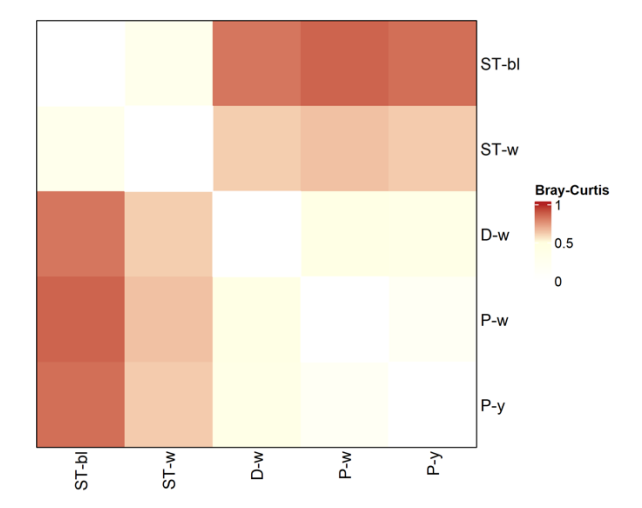
The sequencing data were then stored and re-analysed again in the laboratory by using the lab_pipeline to validate the analyses conducted in the cave. The number of processed reads for each procedure are indicated in Table S4. The results obtained by the two pipelines were compared by applying statistical analyses (Chi-square goodness of fit test), which demonstrated that, for each sample, the results obtained by applying Cave_pipeline and Lab-pipeline were not significantly different considering all the taxonomy levels and including the low abundant taxa (Table S5). This correspondence was strengthened by the very similar values of alpha and beta diversity indexes provided by the analysis of the two datasets (Table S6, Figure S1).

315

4.3.2 Microbial diversity and community composition in silica stromatolite-like samples and other cave biofilms processed in-situ

The sequencing data obtained in the cave were analysed to explore the microbial diversity in the stromatolite samples and in the microbial patina samples collected from the floor.

320 Alpha diversity indexes calculated at different taxonomy levels revealed that D-w, P-w and P-y had higher diversity as compared to the silica stromatolite samples (ST-b and ST-w) (Table S6). Beta-diversity showed that the stromatolite samples were distinct from the three biofilms located on the cave floor in terms of microbial community composition (Figure 10).



325

330

335

Figure 10: Genus level Bray-Curtis dissimilarity matrix between stromatolite (ST-) and biofilm (D-w, P-w, P-y) samples collected from Imawarí Yeutá

By considering the microbial community composition, all the stromatolite and microbial patina samples under analysis were dominated by members of Acidobacteriota phylum and Acidobacteriae class (63-67% in ST-w and ST-b and 41-56% in P-y, P-w and D-w) (Figure S2; Fig. 11). However, there were differences between the two sample groups (stromatolite-like samples vs floor biofilms) at lower taxonomy levels. Indeed, members of Acidobacteriota in samples P-y, P-w and D-w belonged to the orders Subgroup 2 and Acidobacteriales. Despite the high abundance of ASV unclassified at genus level (Table S7), P-y and P-w were enriched by Acidobacteriota genus *Acidipila-Silvibacterium*, while D-w showed higher abundance of *Granulicella* and G12-WMSP1 (Fig. 11). P-y and P-w also showed abundance >1% of the genera *Bryobacter* (*Bryobacteraceae*) and *Candidatus Solibacter* (*Solibacteraceae*). On the contrary, Acidobacteriota members in ST-w and ST-b mostly belonged to Subgroup 13 order unclassified at genus level.

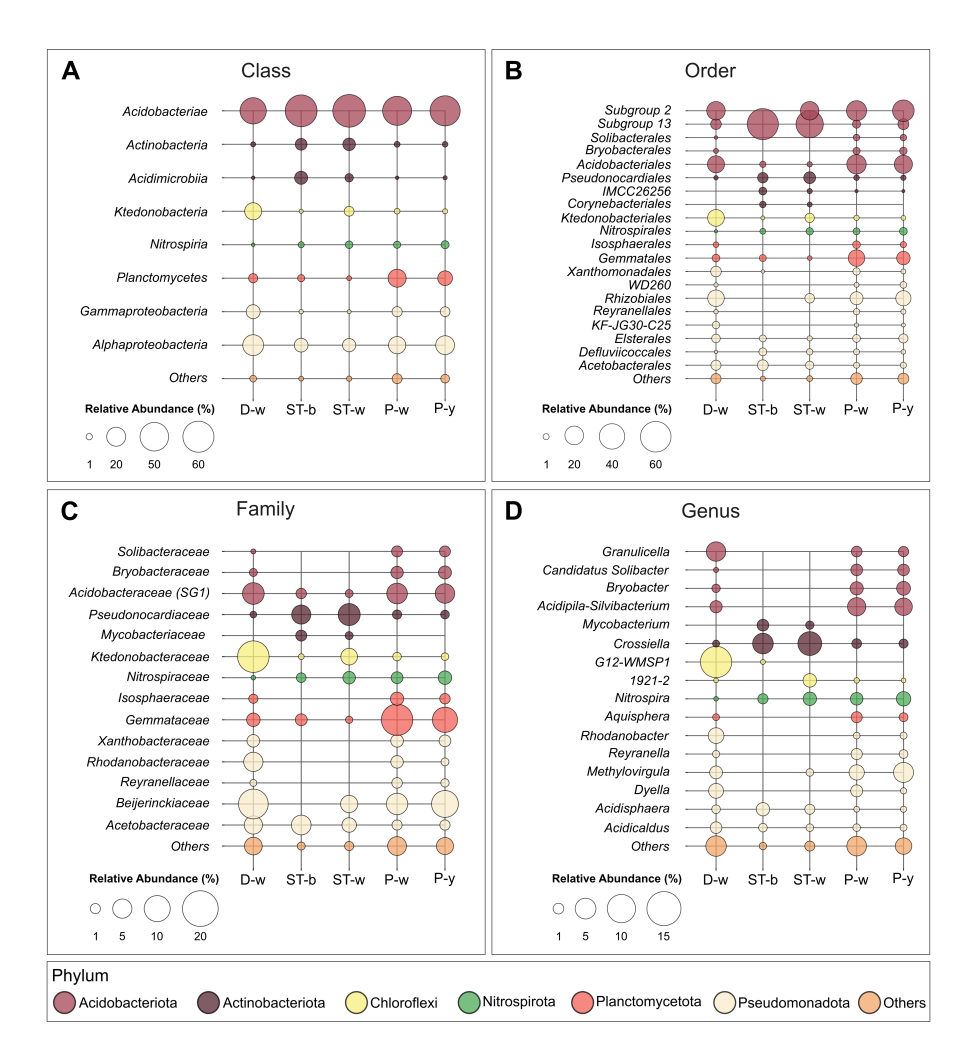


Figure 11: Bubble plot showing the most abundant microbial taxa in each sample at the class (a), order (b), family (c) and genus (d) level. Others include all the taxa with abundance <1%

- After Acidobacteriota, ST-w and ST-b showed the high abundance of Actinobacteriota, which in samples P-y, P-w and D-w were present only in traces (<1%) (Fig. S2). In stromatolite samples, Actinobacteriota members mainly belonged to the family *Pseudonocardiaceae* (Pseudonocardiales order). *Crossiella* (5-7%) was the most abundant genus in both ST-w and ST-b, while *Mycobacterium* was >1% only in ST-b. In the samples P-y, P-w and D-w, the second most abundant phylum was Proteobacteria (20-34%). This phylum mostly included members of *Beijerinckiaceae* family (Rhizobiales) of the class Alphaproteobacteria.
 Members of Gammaproteobacteria showed some differences between the three biofilm samples. In D-w and P-w, Gammaproteobacteria mostly belonged to *Rhodanobacteraceae* family (Xanthomonadales). In P-y, Gammaproteobacteria
 - were mainly represented by the uncharacterized order WD260.

In ST-w and ST-b, the Alphaproteobacteria class (8-9%) was mostly represented by *Acidisphaera* genus (Acetobacteraceaefamily), while *Methylovirgula* genus (*Bejerinkiaceae* family, Rhizobiales order) was present only in ST-w. ST-b showed significant abundance of Defluviicoccales (2.2%) and Elsterales (1.5%) orders, which were not detected in ST-w. Among all the samples, D-w was the only sample where Chloroflexi phylum was abundant (15%), represented mainly by Ktedonobacteria class (14%), Ktedonobacterales order (14%) and Ktedonobacteraceae family (4.5%). Only in the sample ST-w there was also a significant abundance of Choloroflexi (3.9%), mainly of the *Ktedonobacteraceae* family (3.6%) and the uncharacterized genus 1921-2 (1.8%). Lastly, in samples P-y and P-w, members of Planctomycetota were significantly present (11-17%) while in D-w the abundance of this phylum was < 4%. In all the samples, this class was mostly represented by members of Planctomycetes class, Gemmatales order and Gemmataceae family. ST-w and ST-b showed an abundance of members of Nitrospira genus (*Nitrospiraceae* family) similar to P-v and P-w (1-2%), while they were absent in D-w.

5. Discussion

350

355

360

365

370

375

380

In this work, we carried out analyses of microbial diversity, composition and biological activity during a scientific expedition to Imawarí Yeutá, which is one of the most ancient and remote caves on Earth (Sauro et al., 2018). For the microbial diversity and composition, we developed an experimental workflow that makes use of minimal laboratory settings, simplified protocols and lightened computational analyses to conduct the entire DNA-based analysis workflow using Oxford Nanopore sequencing technology. ONT is based on the use of electrical current and biomolecules like DNA can be sequenced thanks to the passage through nanopores that induces specific modification/drops in the electrical current allowing discrimination between different nucleic acids. This sequencing technology is a portable and robust platform that is applicable in remote and extreme environments like Arctic and Antarctic fields (Edwards et al., 2019; Johnson et al., 2017), and the International Space Station (Burton et al., 2020; Castro-Wallace et al., 2017) and in a coal mine (Edwards et al., 2017). These studies mostly focused on the setting of equipment and methods to run the ONT sequencer outside of the lab testing the reliability of the sequencing device in isolated fields. Two previous studies (Latorre-Pérez et al., 2021) also combined DNA sequencing with data analysis in situ (in Tabernas Desert and on a ship in the Atlantic Ocean) for microbial community composition analysis. In our study, we combined the sequencing procedure with data analysis in a remote subterranean environment that required an extremely difficult logistics due to the hard accessibility of the cave associated with the need to use an helicopter to reach the top part of Auvan tepui and the need of using ropes and speleological competence and skills to enter the cave that challenged the transportation of the equipment including the electrical power generator. The pipeline we used in the cave (named cave pipeline) was designed to be easy-to-use. It consisted of a simple shell script that provides the microbial abundance data needed for data analysis and visualization of the results. It was designed to function without relying on a satellite Internet connection (that generally works in remote places on Earth but not in caves) and with a short runtime to accommodate the limited electrical power available due to the complex logistics of the expedition, which made it difficult to transport large fuel supplies. To reduce the computational runtime of the Cave pipeline, the raw sequencing data were basecalled in real-time during the sequencing step using the CPU basecalling "fast mode", and the sequencing output generated from each sample

was subjected to random sub-sampling down to 25%. From a computational point of view, basecalling is considered a major bottleneck in the on-field analysis of nanopore sequencing data because it is typically performed in "high accuracy" or "super accuracy" mode requiring powerful GPUs with high energy consumption to operate at reasonable speeds (Peresini et al., 2021; Xu et al., 2021). The results that we obtained in situ using the cave_pipeline were later confirmed by the sequencing data analysis that we conducted in the lab by using a standard pipeline (Lab_pipeline). The standard pipeline employed the 'super accuracy' basecalling mode on HPC nodes equipped with dedicated GPUs and sufficient RAM/CPUs to process the full sequencing output. This comparative analysis demonstrated the reliability of the sequencing results that we obtained in the cave and the applicability of the Cave_pipeline we developed in this study to other subterranean environments like caves and other remote places.

385

390

395

400

405

410

415

The sequencing data obtained in the cave provided the description of the microbial communities present in the Imawarí Yeutá stromatolites and in additional three microbial biofilms that were collected from the cave floor. The results showed that the microbial communities in the two stromatolite samples were similar between each other and distinct from those present in the biofilms on the floor. The main differences between the microbial communities present in the two stromatolite samples and the three microbial biofilms from different cave floor areas regarded the Actinobacteriota and Acidobacteriota phyla. Actinobacteriota were dominant in stromatolite samples and only in traces in the floor biofilm. The Actinobacteriota members in the stromatolite mostly belong to the families Pseudonocardiaceae and Mycobacteriaceae families and to the genera Crossiella and Mycobacterium. The high presence of these taxa in the stromatolite but not in biofilms present on the cave floor suggest a possible role in the silica amorphization process leading to stromatolite formation. In line with this, previous studies suggested that members of these taxa can be involved in biomineralization, rock weathering and rock solubilization processes in caves also in association with their capacity to establish syntrophic relationships with other bacterial taxa (Boubekri et al., 2021; Cockell et al., 2013; Martin-Pozas et al., 2023). These taxa were also found to possess genetic features associated with atmospheric gases oxidation like H₂ and CO (Ghezzi et al., 2021) that play key roles in biogeochemical cycles and sustain the development of complex microbial communities in oligotrophic environments like Imawarí Yeutá (Nayeli Luis-Vargas et al., 2024). Finally, Crossiella was recently suggested to carry out CO₂ fixation in association with carbonate precipitation leading to carbonate spelothem formation in caves (Martin-Pozas et al., 2023).

Regarding the differences in terms of Acidobacteriota, the stromatolite samples were characterized by members of Subgroup 13, while biofilms on floor showed higher abundance of members of Subgroup 2 and of Acidobacterales of Subgroup 1. This might be associated with the different environmental conditions present in the stromatolite as compared to the surface of quartzite rock substrate on the floor. Indeed, previous studies from our group (Sauro et al., 2019) indicated that the silica amorphization process leading to stromatolite-like structure formation is accompanied by an increase of metals and pH alteration (towards alkalization). This process might drive the enrichment/selection of specific Acidobacteriota lineages as different acidobacterial subgroups respond differently to environmental factors (Naether et al., 2012). Some direct or indirect involvement of Acidobacteriota members in silica biomineralization process could also be hypothesized based on the fact that different members of this phylum are known to i) facilitate mineral solubilization in soil; ii) produce exopolysaccharides

(Kalam et al., 2020) that could function as nucleation sites in mineral precipitation processes; iii) be abundant in cave speleothems like moonmilk (Dhami et al., 2018; Theodorescu et al., 2023), which form through a process of rock solubilization and re-precipition that is similar to silica amorphization occurring in Imawarí Yeutá.

The DNA sequencing analysis and microbial composition study were also accompanied by metabolic activity analyses of the silica stromatolite samples that were conducted directly in the cave using a bioluminometer (ATP detector). This is a portable instrument that allows ATP quantification based on the intensity of bioluminescence that is generated through an enzymatic reaction catalyzed by luciferase. A previous study demonstrated the reliability of this method to estimate metabolically active bacteria (Barton et al., 2014; Chen et al., 2016). Our analyses revealed the presence of higher microbial activity in the white microbial colonies/biofilms present at the interface between the stromatolite and the quartzite rock (ST-w) as compared to the black/greyish patina at the top of the stromatolite (ST-b). These results were later supported by data obtained in the laboratory through qPCR that indicated the presence of higher bacterial cell number in the samples in the white microbial colonies/biofilms. Moreover, the metabolic activity and diversity in these samples were measured in the lab by using Biolog assay that quantifies the NADH produced via bacterial cell oxidation of a large array of substrates. This type of metabolic assay has been extensively used to determine the metabolic potential of microbial communities from different types of environments and in several cases it was used as measurement of functional diversity present in microbial ecosystems (Perujo et al., 2020). In line with the ATP levels we identified in the cave, Biolog assay results obtained in the lab indicated higher metabolic activity levels in the white part of the stromatolite (present at the interface between the stromatolite and rock) as compared to the black/greyish part (on the top of the stromatolite). This result suggests that the stromatolite development is associated with microbial activities that are at the basis of the stromatolite at the interface with the rock. Indeed, the higher metabolic activity might be due to the readily available nutrients solubilized from the quartzite rock/substrate in association to the mineralization processes. Biolog assay results also showed that, differently from the black/greyish patina, the microbial community in white part of stromatolite can metabolize amino acids and amines. These results support a hypothesis described in (Sauro et al., 2018) that associates microbial metabolisms involved in nitrogen compound degradation with the raise of pH observed during silica solubilization processes in Imawarí Yeutá.

6. Conclusions

420

425

430

435

440

445

This work describes the development and validation of procedures to carry out microbial activity/quantification analysis and DNA sequencing in a remote subterranean environment. The results from this study also provide novel insights into the microbiology of silica deposits in orthoquartzite caves, which are considered promising Mars analogues for subsurface and silica-rich environments. The use of Imawarí Yeutá as an environmental setting for these procedures was functional to highlight its potential as an extraterrestrial analogue on Earth, given its extreme remoteness, isolation, and morphological analogies with silica structures detected on Mars. At the same time, it offered scientific interest for studying the microbial communities colonizing this oligotrophic cave and inhabiting the peculiar silica stromatolite-like structures that likely contribute to their

formation. In this context, stromatolite structures could be identified in the speleothems from Imawarí Yeutá through petrological thin sections and SEM images. In-cave and in-lab analyses allowed the assessment of the active role of microbial cells in the process of stromatolite formation and indicated a possible role of Actinobacteriota and Acidobacteriota members in stromatolite development. Finally, metabolic assays indicated a possible key role of nitrogenous compounds in the microbial activities contributing to the formation of the unique silica stromatolite present in Imawarí Yeutá.

455

460

Data availability

The raw sequencing data generated by this study are available under NCBI BioProject PRJNA1262327.

The shell script used to analyse ONT sequencing data and generate the EMU taxonomy abundance tables, along with the R code to replicate the statistical analyses and figures, have been uploaded in Figshare under the DOI: 10.6084/m9.figshare.29514197.

Author contributions

MC: Conceptualization, Methodology, Investigation, Resources, Data Curation, Funding acquisition, Writing - Original Draft, Writing - Review & Editing, Supervision; GB: Methodology, Software, Formal analysis, Validation, Visualization, Writing - Original Draft; AF: Methodology, Software, Formal analysis, Visualization, Writing - Review & Editing; EL: Formal analysis, Investigation, Visualization, Writing - Review & Editing; AC: Investigation, Formal analysis, Visualization, Writing - Review & Editing; FP: Investigation, Writing - Review & Editing; FV: Resources, Writing - Review & Editing; BC: Investigation, Visualization; FS: Investigation, Funding acquisition, Project administration; Writing - Review & Editing.

470

Competing interests

The authors declare that they have no conflict of interest.

Acknowledgments

We acknowledge all members of La Venta Esplorazioni Geografiche and Theraphosa Exploring Team for the support on the field, in particular, Lenin Vargas and Jesus Vergara. We would also like to thank the indigenous community of Kamarata and the Government of Bolivar State for granting the permit to access the cave for speleological research. We thank Dr Maria Roberta Randi for the SEM images realized at the BIGEA Department of the University of Bologna. Finally, we thank the ZDF film crew composed by Lars Abromheit, Jochen Schmoll, Hans Hornberger, Hans Mayr who accompanied us during the expedition to film the scientific expedition. The documentary movie of the expedition (a Gruppe 5 Film produktion production in collaboration with ZDF heute – ARTE) can be watched at the following link: https://www.zdf-studios.com/en/program-catalog/international/unscripted/science-knowledge/tepui-house-gods

Financial support

The 2023 expedition was supported by Tiziano Conte, Loris Greaud Studio, Gruppe5, Ferrino, Tiberino, Amphibious, Insula. The instrumentation was provided by the Bachelor Degree Course in Genomics at the University of Bologna and by Miles Beyond. The microbiological analyses were supported by UNIBO RFO 2020 and 2021. The E.L. PhD scholarship is financed by the funds PNRR-DM118/2023 (a programme funded by NextGeneration EU).

490 References

Aubrecht R, Barrio-Amorós CL and Breure A. Venezuelan Tepuis: Their Caves and Biota. KIP Monogr 2012.

Aubrecht R, Brewer-Carías C, Šmída B, et al. Anatomy of Biologically Mediated Opal Speleothems in the World's Largest Sandstone Cave: Cueva Charles Brewer, Chimantá Plateau, Venezuela. Sediment Geol 2008;203(3–4):181–195; doi: 10.1016/J.SEDGEO.2007.10.005.

- 495 Auler AS and Sauro F. Quartzite and Quartz Sandstone Caves of South America. Encycl Caves, Third Ed 2019;850–860; doi: 10.1016/B978-0-12-814124-3.00102-3.
 - Barton HA, Giarrizzo JG, Suarez P, et al. Microbial Diversity in a Venezuelan Orthoquartzite Cave Is Dominated by the Chloroflexi (Class Ktedonobacterales) and Thaumarchaeota Group I.1c. Front Microbiol 2014;5(NOV); doi: 10.3389/fmicb.2014.00615.
- Boston PJ. Location, Location! Lava Caves on Mars for Habitat, Resources, and the Search for Life. J Cosmol 2010;12:3957–3979.
 - Boubekri K, Soumare A, Mardad I, et al. The Screening of Potassium- and Phosphate-Solubilizing Actinobacteria and the Assessment of Their Ability to Promote Wheat Growth Parameters. Microorganisms 2021;9(3):1–16; doi: 10.3390/MICROORGANISMS9030470.
- 505 Burton AS, Stahl SE, John KK, et al. Off Earth Identification of Bacterial Populations Using 16S RDNA Nanopore Sequencing. Genes 2020, Vol 11, Page 76 2020;11(1):76; doi: 10.3390/GENES11010076.
 - Castro-Wallace SL, Chiu CY, John KK, et al. Nanopore DNA Sequencing and Genome Assembly on the International Space Station. Sci Reports 2017 71 2017;7(1):1–12; doi: 10.1038/s41598-017-18364-0.
- Chen Z, Liu Y, Wei H, et al. Tube Coalescence in the Jingfudong Lava Tube and Implications for Lava Flow Hazard of Tengchong Volcanism. Int J Speleol 2016;45(3):219–229; doi: 10.5038/1827-806X.45.3.1987.
 - Cockell CS, Kelly LC and Marteinsson V. Actinobacteria-An Ancient Phylum Active in Volcanic Rock Weathering. Geomicrobiol J 2013; doi: 10.1080/01490451.2012.758196.
 - Curry KD, Wang Q, Nute MG, et al. Emu: Species-Level Microbial Community Profiling for Full-Length Nanopore 16S Reads. Nat Methods 2022;19(7):845; doi: 10.1038/S41592-022-01520-4.
- 515 Daza Brunet R and Bustillo Revuelta MÁ. Exceptional Silica Speleothems in a Volcanic Cave: A Unique Example of

- Silicification and Sub-Aquatic Opaline Stromatolite Formation (Terceira, Azores). Sedimentology 2014;61(7):2113–2135; doi: 10.1111/SED.12130.
- Dhami NK, Mukherjee A and Watkin ELJ. Microbial Diversity and Mineralogical-Mechanical Properties of Calcitic Cave Speleothems in Natural and in Vitro Biomineralization Conditions. Front Microbiol 2018;9:40; doi: 10.3389/FMICB.2018.00040/FULL.
- Edwards A, Debbonaire AR, Nicholls SM, et al. In-Field Metagenome and 16S RRNA Gene Amplicon Nanopore Sequencing Robustly Characterize Glacier Microbiota. bioRxiv 2019;073965; doi: 10.1101/073965.
 - Edwards A, Soares A, Rassner SME, et al. Deep Sequencing: Intra-Terrestrial Metagenomics Illustrates the Potential of off-Grid Nanopore DNA Sequencing. bioRxiv 2017;133413; doi: 10.1101/133413.
- Ghezzi D, Foschi L, Firrincieli A, et al. Insights into the Microbial Life in Silica-Rich Subterranean Environments: Microbial Communities and Ecological Interactions in an Orthoquartzite Cave (Imawarì Yeuta, Auyan Tepui, Venezuela). Front Microbiol 2022;13:930302; doi: 10.3389/FMICB.2022.930302/FULL.
 - Ghezzi D, Sauro F, Columbu A, et al. Transition from Unclassified Ktedonobacterales to Actinobacteria during Amorphous Silica Precipitation in a Quartzite Cave Environment. Sci Rep 2021;11(1):3921; doi: 10.1038/S41598-021-83416-5.
- Gunnarsson I and Arnórsson S. Amorphous Silica Solubility and the Thermodynamic Properties of H4SiO°4 in the Range of 0° to 350°C at Psat. Geochim Cosmochim Acta 2000;64(13):2295–2307; doi: 10.1016/S0016-7037(99)00426-3.
 - Insam H. A New Set of Substrates Proposed for Community Characterization in Environmental Samples. Microb Communities 1997;259–260; doi: 10.1007/978-3-642-60694-6 25.
 - Johnson SS, Zaikova E, Goerlitz DS, et al. Real-Time DNA Sequencing in the Antarctic Dry Valleys Using the Oxford
- 535 Nanopore Sequencer. J Biomol Tech 2017;28(1):2–7; doi: 10.7171/JBT.17-2801-009.
 - Kalam S, Basu A, Ahmad I, et al. Recent Understanding of Soil Acidobacteria and Their Ecological Significance: A Critical Review. Front Microbiol 2020;11; doi: 10.3389/FMICB.2020.580024.
 - Konhauser KO, Jones B, Phoenix VR, et al. The Microbial Role in Hot Spring Silicification. Ambio 2004;33(8):552–558; doi: 10.1579/0044-7447-33.8.552,.
- Latorre-Pérez A, Gimeno-Valero H, Tanner K, et al. A Round Trip to the Desert: In Situ Nanopore Sequencing Informs Targeted Bioprospecting. Front Microbiol 2021;12; doi: 10.3389/FMICB.2021.768240.
 - Lundberg J, Brewer-Carías C and McFarlane DA. On Biospeleothems from a Venezuelan Tepui Cave: U-Th Dating, Growth Rates, and Morphology. Int J Speleol 2018;47(3):6; doi: https://doi.org/10.5038/1827-806X.47.3.2212.
 - Maggiori C, Stromberg J, Blanco Y, et al. The Limits, Capabilities, and Potential for Life Detection with MinION Sequencing
- 545 in a Paleochannel Mars Analog. Astrobiology 2020;20(3):375–393; doi: 10.1089/AST.2018.1964/ASSET/IMAGES/AST.2018.1964 FIGURE9.JPG.
 - Martin-Pozas T, Gonzalez-Pimentel JL, Jurado V, et al. Crossiella, a Rare Actinomycetota Genus, Abundant in the Environment. Appl Biosci 2023;2(2):194–210; doi: 10.3390/applbiosci2020014.
 - Mecchia M, Sauro F, Piccini L, et al. Geochemistry of Surface and Subsurface Waters in Quartz-Sandstones: Significance for

- the Geomorphic Evolution of Tepui Table Mountains (Gran Sabana, Venezuela). J Hydrol 2014;511:117–138; doi: 10.1016/j.jhydrol.2014.01.029.
 - Miller AZ, Pereira MFC, Calaforra JM, et al. Siliceous Speleothems and Associated Microbe-Mineral Interactions from Ana Heva Lava Tube in Easter Island (Chile). Geomicrobiol J 2014; doi: 10.1080/01490451.2013.827762.
- Mojarro A, Hachey J, Bailey R, et al. Nucleic Acid Extraction and Sequencing from Low-Biomass Synthetic Mars Analog
- 555 Soils for In Situ Life Detection. Astrobiology 2019;19(9):1139–1152; doi: 10.1089/AST.2018.1929.
 - Naether A, Foesel BU, Naegele V, et al. Environmental Factors Affect Acidobacterial Communities below the Subgroup Level in Grassland and Forest Soils. Appl Environ Microbiol 2012;78(20):7398–7406; doi: 10.1128/AEM.01325-12/SUPPL FILE/ZAM999103757SO1.PDF.
 - Nayeli Luis-Vargas M, Webb J, White S, et al. Linking Surface and Subsurface: The Biogeochemical Basis of Cave Microbial
- 560 Ecosystem Services. J Sustain Agric Environ 2024;3(4):e70031; doi: 10.1002/SAE2.70031;WGROUP:STRING:PUBLICATION.
 - O'Connor BRW, Fernández-Martínez MÁ, Léveillé RJ, et al. Taxonomic Characterization and Microbial Activity Determination of Cold-Adapted Microbial Communities in Lava Tube Ice Caves from Lava Beds National Monument, a High-Fidelity Mars Analogue Environment. Astrobiology 2021;21(5):613–627; doi: 10.1089/AST.2020.2327,.
- Peresini P, Boza V, Brejova B, et al. Nanopore Base Calling on the Edge. Bioinformatics 2021;37(24):4661; doi: 10.1093/BIOINFORMATICS/BTAB528.
 - Perujo N, Romaní AM and Martín-Fernández JA. Microbial Community-Level Physiological Profiles: Considering Whole Data Set and Integrating Dynamics of Colour Development. Ecol Indic 2020;117:106628; doi: 10.1016/J.ECOLIND.2020.106628.
- Quintela IA, Vasse T, Lin CS, et al. Advances, Applications, and Limitations of Portable and Rapid Detection Technologies for Routinely Encountered Foodborne Pathogens. Front Microbiol 2022;13:1054782; doi: 10.3389/FMICB.2022.1054782.
 Ruff SW and Farmer JD. Silica Deposits on Mars with Features Resembling Hot Spring Biosignatures at El Tatio in Chile.
 Nat Commun 2016;7:13554; doi: 10.1038/ncomms13554.
- Ruff SW, Farmer JD, Calvin WM, et al. Characteristics, Distribution, Origin, and Significance of Opaline Silica Observed by the Spirit Rover in Gusev Crater, Mars. J Geophys Res E Planets 2011; doi: 10.1029/2010JE003767.
 - Sauro F. Structural and Lithological Guidance on Speleogenesis in Quartz-Sandstone: Evidence of the Arenisation Process. Geomorphology 2014;226:106–123; doi: 10.1016/j.geomorph.2014.07.033.
 - Sauro F, Cappelletti M, Ghezzi D, et al. Microbial Diversity and Biosignatures of Amorphous Silica Deposits in Orthoquartzite Caves. Sci Rep 2018;8(1):1–14; doi: 10.1038/s41598-018-35532-y.
- 580 Sauro F, Lundberg J, De Waele J, et al. Speleogenesis and Speleothems of the Guacamaya Cave , Auyan Tepui , Venezuela. 2013.
 - Sauro F, Mecchia M, Piccini L, et al. Genesis of Giant Sinkholes and Caves in the Quartz Sandstone of Sarisariñama Tepui, Venezuela. Geomorphology 2019;342:223–238; doi: 10.1016/j.geomorph.2019.06.017.

- Sauro F, Onac BP, Carbone C, et al. Secondary Cave Minerals and Sedimentary Deposits in Orthoquartzite and Metaquartzite

 Caves of South America: A Review on Their Genesis and Significance. In: 18th International Congress of Speleology 2022.

 Sauro F, Tisato N, De Waele J, et al. Source and Genesis of Sulphate and Phosphate-Sulphate Minerals in a Quartz-Sandstone

 Cave Environment. Sedimentology 2014;61(5):1433–1451; doi: 10.1111/sed.12103.
 - Smith MR, Bandfield JL, Cloutis EA, et al. Hydrated Silica on Mars: Combined Analysis with near-Infrared and Thermal-Infrared Spectroscopy. Icarus 2013;223(2):633–648; doi: 10.1016/J.ICARUS.2013.01.024.
- Theodorescu M, Bucur R, Bulzu PA, et al. Environmental Drivers of the Moonmilk Microbiome Diversity in Some Temperate and Tropical Caves. Microb Ecol 2023;86(4):2847–2857; doi: 10.1007/S00248-023-02286-8.
 - Wray RAL and Sauro F. An Updated Global Review of Solutional Weathering Processes and Forms in Quartz Sandstones and Quartzites. Earth-Science Rev 2017;171:520–557; doi: 10.1016/J.EARSCIREV.2017.06.008.
- Xu Z, Mai Y, Liu D, et al. Fast-Bonito: A Faster Deep Learning Based Basecaller for Nanopore Sequencing. Artif Intell Life Sci 2021;1:100011; doi: 10.1016/J.AILSCI.2021.100011.